Toward an Accurate Estimate of the Exfoliation Energy of Black Phosphorus: A Periodic Quantum Chemical Approach

(Article begins on next page)

05 May 2024

Towards an Accurate Estimate of the Exfoliation Energy of Black Phosphorus: A Periodic Quantum Chemical Approach

Giuseppe Sansone[1],* Lorenzo Maschio[1], Denis Usvyat[2],* Martin Schütz[2], and Antti Karttunen[3]*

[1]*Dipartimento di Chimica and NIS (Nanostructured Interfaces and Surfaces) Centre, Università di Torino, via Giuria 5, I-10125 Torino, Italy*

[2] *Institute for Physical and Theoretical Chemistry, University of Regensburg, Universitätsstraße 31, D-93040 Regensburg (Germany)*

[3]*Department of Chemistry, Aalto University, Kemistintie 1, 02150 Espoo, Finland*

E-mail: giuseppe.sansone@unito.it; denis.usvyat@chemie.uni-regensburg.de; antti.j.karttunen@iki.fi

Abstract

The Black phosphorous (black-P) crystal is formed of covalently bound layers of phosphorene stacked together by weak van der Waals interactions. An experimental measurement of the exfoliation energy of black-P is not available presently, making theoretical studies the most important source of information for the optimization of phosphorene production. Here, we provide an accurate estimate of the exfoliation energy of black-P on the basis of multilevel quantum chemical calculations, which include the periodic local Møller-Plesset perturbation theory of second order, augmented by higher-order corrections, which are evaluated with finite clusters mimicking the crystal.

Very similar results are also obtained by density functional theory with the D3-version of Grimme's empirical dispersion correction.

Our estimate of the exfoliation energy for black-P of -151 meV/atom is substantially larger than that of graphite, suggesting the need for different strategies to generate isolated layers for these two systems.

Phosphorus is well known for its ability to form a variety of allotropes in the solid state. In this respect it closely resembles carbon, whose nanostructures (0D-fullerenes, 1D-nanotubes, 2D-graphene) have led to the impressive development of nanoscience in recent years. Solid phases of phosphorus, although known since long, are studied nowadays with a renewed interest,[1] as precursors of nanostructures analogous to carbon-based ones. Among the graphene[2,3]-inspired 2D materials, such as silicene,[4] germanene[4] and stanene,[5] phosphorene has been very recently fabricated[6,7] and proposed as a candidate for future electronics, optoelectronics, photovoltaics and spintronics applications.[8,9] A systematic development of new modifications and applications of phosphorene requires a complete understanding of structure and energetics of its parent crystal, *i.e.*, black phosphorus (black-P). The latter is the most stable allotrope of phosphorus,[10,11] and is built from an infinite stacking of phosphorene layers, *cf.* Figure 1.

Notably, a detailed understanding of the interactions in black-P can show new ways to fabricate high-quality phosphorene samples and novel phosphorene-based technologies. From a computational point of view, black-P is a very challenging system because of the simultaneous presence of covalent (intralayer) and weak dispersive (interlayer) forces. It is well-known that Kohn-Sham density functional theory (DFT)[12,13] utilizing commonly used approximations of the exchange correlation functional is unable to properly describe van der Waals interactions.[14] Nonempirical van der Waals functionals,[15–17] dispersion-corrected atom-centered potentials (DCACPs)[18], and Grimme's empirical dispersion corrections[19–21] offer a practical solution to that problem. Yet, they typically rely on some form of parametrization and may therefore fail unexpectedly. Computational studies of solid phosphorus using such DFT
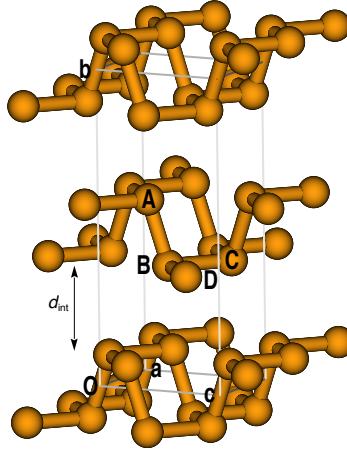
Figure 1: The black phosphorus crystal structure is built from phosphorene layers. The "chair" interconnection of the six-membered rings gives rise to the characteristic puckered shape of the layers. Lowercase letters (a,b,c) refer to the lattice parameters. Along the direction of the **b** lattice vector, the interlayer distance (d_{int}) is depicted. Uppercase letters (A,B,C,D) have been used to define the so-called hinge angle ($\angle CBD$) and the adjacent P–P bond length (d_{BC}), the dihedral angle ($\angle ABC$), and the connecting bond length (d_{AB}).

approaches and Quantum Monte Carlo methods are found in the recent literature.[8,22–26] Nevertheless, when looking for a reliable estimate of a physical quantity, accurate *ab initio* wavefunction methods are indispensable tools since they can be employed to assess and rank the quality of different DFT approaches for a given system. Post-HF approaches, as employed in this work, have already provided important insight into the formation of other allotropes of phosphorus, such as that of red of phosphorus, where systematic MP2 studies on phosphorus clusters have been perfomed already over 20 years ago.[27]

Here we apply periodic local second-order Møller-Plesset perturbation theory (p-LMP2)[28–30] to study the interlayer interactions between the phosphorene layers in black-P, which is corrected for basis set and method errors by using finite cluster calculations. These results are compared to those obtained from different flavours of dispersion-corrected DFT. Post-Hartree-Fock (HF) calculations on crystalline solids within the periodic theoretical framework are nowadays still not yet routine.[31–33] For the present study the recent developments in

3

the p-LMP2 method,[34] such as the implementation of orbital-specific virtuals (OSV),[35] were very instrumental, since they substantially simplify calculation of smooth potential energy surfaces (*vide infra*).

Following a computational protocol, recently proposed for molecular crystals,[36] and adsorption on surfaces[37,38] we have evaluated finite cluster corrections accounting for the method and basis-set errors as well as the neglect of core-electron correlations. The corrections are computed by using the interaction energies of the $P_4H_6 - P_{16}H_{10}$ dimer (see supplementary information), cut out from the crystal structure within the given interlayer distance, with the dangling bonds substituted by P-H ones. The correcting energy increments are evaluated as the differences in interaction energies on top of the OSV-LMP2 (or OSV-spin-component-scaled-LMP2, see below) results. The high-end quantum chemical treatment reaches the coupled cluster with singles, doubles and perturbative triples CCSD(T) level (often considered the "gold standard" of quantum chemistry) in a reasonably large basis set, *i.e.*, of augmented triple zeta quality. Due to the relatively large size of the dimer, local[39,40], rather than canonical CCSD(T) calculations are performed. To this end we utilize the LCCSD(T0)|LCCD[S]-R^{-6} method.[41,42] This local approximation to the CCSD(T) method provides a very high accuracy for intermolecular systems.[42]

MP2 is notorious for overestimating dispersion for highly polarizable systems. As will be clear from the results presented below, this is also the case for black-P (which is a small band gap semiconductor), if an extended and diffuse basis set is used. For such systems, the spin-component-scaled(SCS)-MP2[43] technique is known to be much more stable and closer to CCSD(T). Therefore we evaluate the basis set and CCSD(T) corrections with respect to the periodic OSV-SCS-LMP2 treatment. For brevity, we denote in the following the sum of all the three corrections, *i.e.*, method, basis set, and core correlation, by the one acronym ΔCCSD(T).

All calculations have been performed by using the CRYSTAL[44] program for HF and DFT, and CRYSCOR[30] for p-LMP2, and MOLPRO[45] for the LCCSD(T) calculations and other

cluster corrections. All these codes employ a basis set of atom-centered Gaussian-type orbitals. In periodic calculations we used basis sets derived from the molecular Karlsruhe basis sets[46] (see Supporting Information – SI – for details). We applied basis sets of different quality: split-valence plus polarization (SVP) and triple-zeta-valence with three different sets of polarization functions (TZVP with 1d; TZVPP with (2d1f)[2d1f] and TZVPP2 with (3d1f)[2d1f]). Finally, in the periodic LMP2 and SCS-LMP2 calculations for determining the exfoliation energy we augmented the TZVPP2 basis with diffuse d- and f-orbitals from Dunning's aug-cc-PVTZ basis set,[47] which are essential for an accurate description of dispersion.[38,48] Since such diffuse orbitals are harmful for periodic HF, they were added only *a posteriori* for the correlated calculations by means of the dual basis set technique.[29] The finite cluster corrections were computed using basis sets from the Dunning family, *i.e.*, aug-cc-pVTZ for the CCSD(T) - SCS-LMP2 energy difference; (ii) aug-cc-pVTZ and aug-cc-pVQZ for the basis set extropolation at the SCS-MP2 level; (iii) aug-cc-pwCVTZ[49] for the correlated core correction.

As a first step, we optimised the cell parameters of black-P at the p-LMP2 level. Since p-LMP2 analytical nuclear gradients are presently not available in the CRYSCOR code, we sampled the potential energy surface through single point calculations on a 3D grid around the experimental structure. Five symmetry irreducible geometrical parameters need to be optimised for black-P: three lattice parameters (a, b, c) and two fractional coordinates of the atoms (y/b and z/c). We tackled these cell and atomic coordinates separately.

2D potential energy surfaces were then obtained from fitting a quadratic function at each b value to the corresponding subset of data points. Figure 2 shows an example of such a fitting. For more details on the fit see SI. The resulting potential energy surface is indeed smooth. Such smoothness is not automatically achieved in the local correlation approach, based on projected atomic orbitals,[28] due to a possible domain mismatch along the potential surface scan. However, the recent implementation of the OSV-based p-LMP2[34] to a large extent eliminates this problem.
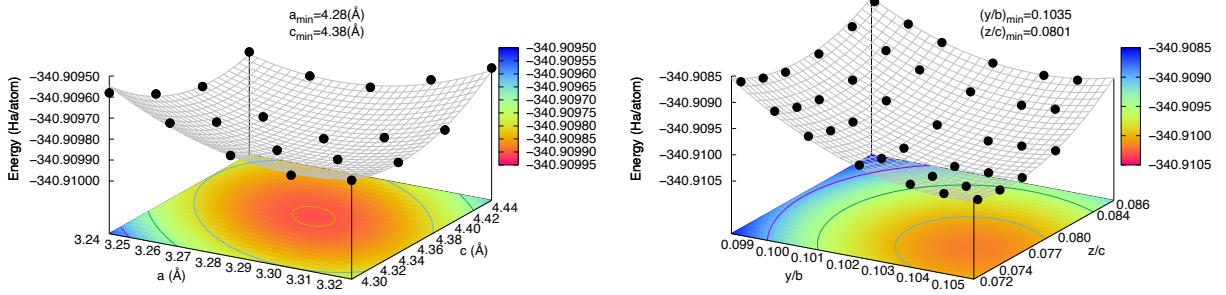
Figure 2: Potential energy surface of black-P fitted to explicitly computed energies at the p-LMP2/TZVPP level of theory. Left Panel: Energy as a function of a and c cell parameters (with fixed $b = 10.38$ Å). Right Panel: Energy as a function of the internal coordinates of the phosphorus atoms in the fractional units y/b and z/c, with fixed $x/a = 0$.

Note that the lattice parameter b corresponds to the stacking direction, and both inter-layer distance and layer thickness are related to it. Note that the change in the latter, which also involves contraction or elongation of the P-P bonds, corresponds to a "hard" coordinate (with large curvature of the potential energy surface along this direction). On the other hand, the interlayer distance is a typical "weak" coordinate. Therefore, the lattice parameter b strongly couples these hard and weak coordinates. The so "optimized" b-parameter value hence is governed by the hard coordinate.

In order to decouple the inter– from the intra-layer interaction, we computed a one-dimensional potential energy profile in which all coordinates were frozen at the previously found minimum, and only the interlayer distance d_{int} was varied. Futhermore, here we focused directly on the exfoliation energy, which allowed us not only to elminate the basis set superposition error for this delicate quantity, but also to incorporate the finite cluster ΔCCSD(T) corrections into the potential energy curve. The counterpoise corrected exfolia-tion energy is given by the expression:

$$E_{\mathrm{exf}} = E_{\mathrm{bulk}} - E_{\mathrm{lay}}^{\mathrm{gh}} + \Delta E_{\mathrm{relax}}, \tag{1}$$

6

where E_{bulk} and $E_{\mathrm{lay}}^{\mathrm{gh}}$ are the total energy of the bulk black-P and the total energy of a single layer of black-P in the bulk geometry with ghost functions on the two nearest-neighboring layers, respectively (both in energies are per atom). The relaxation energy for the single layer

$$\Delta E_{\mathrm{relax}} = E_{\mathrm{lay}} - E_{\mathrm{lay}}^{\mathrm{opt}}, \tag{2}$$

involves the total energies (also per atom) of the isolated layer in the bulk (E_{lay}) and the optimized ($E_{\mathrm{lay}}^{\mathrm{opt}}$) geometries. In the absence of periodic LMP2 nuclear gradients, the optimization of the layer, as well as the evaluation of $\Delta E_{\mathrm{relax}}$ was done at the PBE0-D3 level.

First, in Table 1 we report the optimized (according to the described scheme) p-LMP2 lattice parameters for the TZVPP and TZVPP2 basis sets and compare them to the fully optimized (cell parameters and fractional coordinates) values from two DFT functionals PBE[52] and PBE0[53] with and without dispersions corrections D2[19] and D3.[21] From these results several observations can be made:

(i) Van der Waals forces are crucial for a correct description of black-P. A wide range of values for the b parameter is obtained by the different functionals. The PBE and PBE0 functionals with no dispersion corrections tend to substantially overestimate the cell volume.

(ii) The better performance of the plain PBE or PBE0 functionals in conjunction with smaller basis sets (compared to saturated basis sets) is due to basis set superposition error (BSSE) effects that act as spurious attractive interaction between the layers.

(iii) The agreement with experiment of the dispersion corrected DFT and LMP2 is very good as far as a and c are concerned. For the b parameter only DFT-D2 gives a result close to the experimental value. We note, that in previous works it was shown that the D3 correction can generally be expected to be superior to D2,[54] even though weak interactions are overestimated.[55,56] Here we see that both DFT-D3 and LMP2 similarly provide a noticeably smaller value for b than DFT-D2 as well as the experiment. At the same time, experimental values corresponds to room temperature and therefore it remains unclear if it can be regarded as a proper reference for the electronic-energy-only optimization of the b parameter.

Table 1: Summary of the black-P structural data obtained from the p-LMP2 and DFT structure optimisations. The relaxed cell parameters (a, b, c) and inter-layer distance (d_{int}) have been compared with two experimental studies.

Method	Basis set	a (Å)	b (Å)	c (Å)	V (Å^3/atom)	d_{int} (Å)	b (Å)	V (Å^3/atom)	d_{int} (Å)
							BSSE-corrected values		
Exp. 1[50]		3.31	10.48	4.38	19.0	3.11			
Exp. 2[51]		3.31	10.47	4.37	19.0	3.07			
p-LMP2	TZVPP	3.28	9.88	4.38	17.7	2.79	10.29	18.5	3.00
	TZVPP2	3.27	9.98	4.36	17.8	2.83	10.20	18.2	2.95
PBE	SVP	3.36	10.33	4.35	18.9	2.97			
	TZVP	3.36	10.48	4.45	19.6	3.05			
	TZVPP	3.33	10.64	4.48	19.8	3.16			
	TZVPP2	3.31	10.97	4.51	20.5	3.36			
PBE-D2	SVP	3.36	10.19	4.31	18.5	2.90			
	TZVP	3.37	10.27	4.37	18.9	2.95			
	TZVPP	3.34	10.34	4.41	19.0	3.01	10.42	19.2	3.05
	TZVPP2	3.32	10.42	4.41	19.1	3.07	10.46	19.1	3.09
PBE-D3	SVP	3.36	9.95	4.07	17.0	2.76			
	TZVP	3.36	9.99	4.14	17.4	2.79			
	TZVPP	3.33	10.07	4.15	17.4	2.85	10.15	17.5	2.89
	TZVPP2	3.31	10.13	4.14	17.4	2.89	10.14	17.4	2.90
PBE0	SVP	3.33	10.30	4.36	18.7	3.00			
	TZVP	3.33	10.46	4.45	19.4	3.09			
	TZVPP	3.31	10.62	4.49	19.7	3.20			
	TZVPP2	3.29	10.94	4.50	20.2	3.38			
PBE0-D2	SVP	3.34	10.16	4.33	18.4	2.93			
	TZVP	3.34	10.24	4.39	18.8	2.98			
	TZVPP	3.32	10.32	4.42	18.9	3.04	10.42	19.1	3.09
	TZVPP2	3.30	10.42	4.42	19.0	3.11	10.48	19.1	3.14
PBE0-D3	SVP	3.33	9.91	4.17	17.2	2.80			
	TZVP	3.33	9.98	4.21	17.5	2.83			
	TZVPP	3.30	10.09	4.25	17.7	2.91	10.19	17.9	2.96
	TZVPP2	3.28	10.17	4.23	17.6	2.97	10.17	17.6	2.97

All computed data are for 0 K, thermal expansion has not been considered.
Experimental data obtained at room temperature.

In order to investigate this discrepancy in more detail we focus on the exfoliation energy as a function of d_{int}. ΔE_{exf}, computed at different levels, is presented in Fig. 3. Importantly, here we have access to a very accurate reference, obtained by adding ΔCCSD(T) to the periodic SCS-LMP2/aug(d,f)-TZVPP2 result.
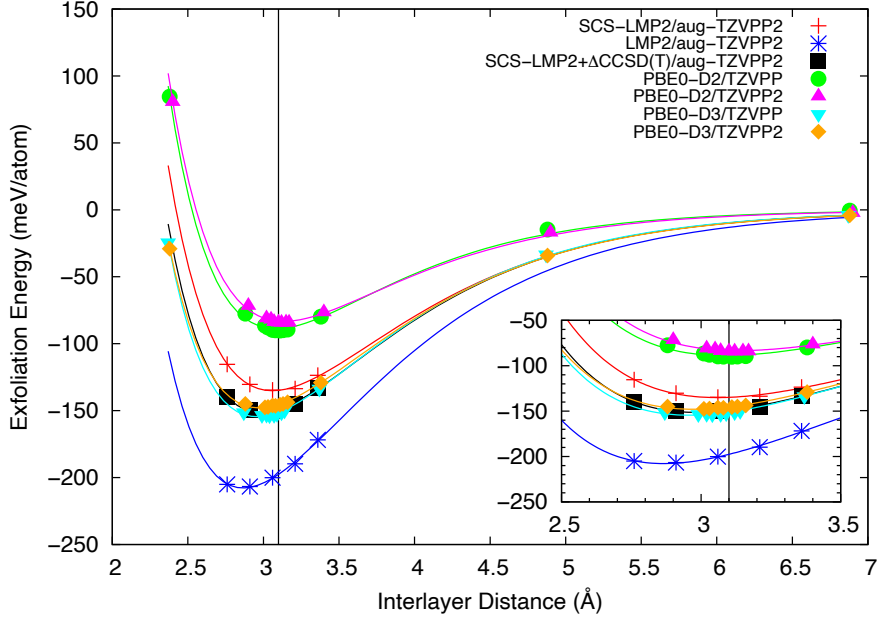

Figure 3: Plot of the exfoliation energy as a function of the interlayer distance in bulk black-P, as evaluated with different methods. Curves have been fitted with a 1D Morse potential. The curves are qualitatively comparable to graphite studied using Quantum Monte Carlo (Spanu *et al.*[57]), but the absolute value of the exfoliation energy is clearly larger for black-P.

First we see from Fig. 3 that the electronic-energy minimum in the reference curve is rather close to that of DFT-D3 and LMP2 with TZVPP2 basis, hence is shifted to *smaller* d_{int} relative to the experimental and DFT-D2 values. At the same time we note an extreme shallowness of the potential curve for a wide range of d_{int} values and thus of the lattice parameter b. This indicates that the thermal expansion of the lattice parameter b can be appreciable in black-P. The experimental linear thermal expansion coefficient in the b-direction is 39×10^{-6} 1/K at room temperature[10]. It is about 1.5 times larger than that of graphite (25×10^{-6} 1/K at room temperature)[58] and implies a small but not negligible change in the b-parameter with temperature. The thermal expansion thus can be a reason

for the discrepancy between the best theoretical and the experimental results. Considering this, the DFT-D2 minimum is likely to be incorrect, despite the good agreement with the experimental structural parameters obtained at the room temperature. In this respect, a theoretical modeling of the thermal expansion of black-P appears is very interesting and will be explored in future work.

As noted above the LMP2 with extended and diffuse basis substantially overestimates binding. Smaller basis sets, especially TZVPP, provide a reasonably good description due to a cancellation of method error *vs.* basis set error. The SCS-LMP2 method, on the contrary, provides a quite accurate interaction energy for black-P only with a sufficiently large basis set.

The exfoliation energy of a layered material such as black-P is equal to the interlayer binding energy (also known as interlayer cohesive energy) and an understanding of the energetics of the interlayer bonding in the layered compounds is fundamental for optimizing their exfoliation processes.[59] Notably, for black-P, a controllable exfoliation process could be exploited to produce few-layer phosphorene systems with a tunable band gap.[60] In other words, few-layer phosphorene is a semiconductor with a finite gap, which is strongly affected by the number of layers, making it highly attractive for applications in, e.g., optoelectronics. However, apart from the archetypal graphite/graphene case[61–63], experimental data on exfoliation energies are very rarely available for weakly bonded layered inorganic compounds.[59] In particular, no experimental estimate on the exfoliation energy of black-P has been reported, to our knowledge. For this reason, an accurate estimate of such quantity is of fundamental importance for a better understanding of the physico-chemical properties of the black-P/phosphorene system at the nanoscale.

The results for the exfoliation energy for Black-P are compiled in the Table 2. PBE-D2 and PBE0-D2 predict it to be around -90 to -100 meV per atom. Similar values for the DFT-D2 exfoliation energy have recently been obtained in Refs.[25,26]. However, both

Table 2: The exfoliation energy (E_{exf}) of black-P calculated using different approaches and corrections. E_{exf} has been calculated from Eq. (1).

Method	Basis set	b (Å)	d_{int} (Å)	E_{exf} (meV/atom)
p-LMP2	TZVPP	10.29	3.00	-158
	TZVPP2	10.20	2.95	-184
p-LMP2	aug(d,f)-TZVPP2	10.05	2.87	-208
p-SCS-LMP2	aug(d,f)-TZVPP2	10.43	3.06	-135
p-SCS-LMP2+ΔCCSD(T)[a]	**aug(d,f)-TZVPP2/cbs**[a]	**10.27**	**2.98**	**-151**
PBE-D2	TZVPP	10.42	3.05	-89
	TZVPP2	10.46	3.09	-84
PBE0-D2	TZVPP	10.42	3.09	-89
	TZVPP2	10.48	3.14	-83
PBE-D3	TZVPP	10.15	2.89	-144
	TZVPP2	10.14	3.90	-139
PBE0-D3	TZVPP	10.19	2.96	-155
	TZVPP2	10.17	2.97	-148

[a] Includes finite-cluster corrections for the method, basis set errors and the core-valence correlation.

p-SCS-LMP2+CCSD(T) and DFT-D3 provide a much stronger interaction in the range of about -140 to -160 meV/atom. Since this estimate is predicted by a sophisticated high-level quantum chemical treatment and is furthermore supported by DFT with the most recent parameterization of the dispersion correction, we consider it as the most accurate benchmark so far for the electronic contribution to the exfoliation energy of black-P.

For graphite, the exfoliation energy has been estimated to be in the range of -30 to -50 meV per atom.[61–63] Hence, the predicted exfoliation energy of black-P is considerably larger than that of graphite. Such a substantial difference in the inter-layer energetics between black-P and graphite suggests that the optimal exfoliation strategies for these two systems might be quite different.

Acknowledgement

Supporting Information Available

This material is available free of charge via the Internet at `http://pubs.acs.org/`.

References

(1) Pfitzner, A. Phosphorus Remains Exciting! *Angew. Chem. Int. Ed.* **2006**, *45*, 699–700.

(2) Katsnelson, M. I. Graphene: Carbon in Two Dimensions. *Mater. Today* **2007**, *10*, 20–27.

(3) Geim, A. K.; Novoselov, K. S. The Rise of Graphene. *Nat. Mater.* **2007**, *6*, 183–191.

(4) Houssa, M.; Scalise, E.; Sankaran, K.; Pourtois, G.; Afanas'ev, V. V.; Stesmans, A. Electronic Properties of Hydrogenated Silicene and Germanene. *Appl. Phys. Lett.* **2011**, *98*, 223107.

(5) Xu, Y.; Yan, B.; Zhang, H.-J.; Wang, J.; Xu, G.; Tang, P.; Duan, W.; Zhang, S.-C. Large-Gap Quantum Spin Hall Insulators in Tin Films. *Phys. Rev. Lett.* **2013**, *111*, 136804.

(6) Li, L.; Yu, Y.; Ye, G. J.; Ge, Q.; Ou, X.; Wu, H.; Feng, D.; Chen, X. H.; Zhang, Y. Black Phosphorus Field-Effect Transistors. *Nat. Nanotechnol.* **2014**, *9*, 372–377.

(7) Liu, H.; Neal, A. T.; Zhu, Z.; Luo, Z.; Xu, X.; Tomànek, D.; Ye, P. D. Phosphorene: An Unexplored 2D Semiconductor With a High Hole Mobility. *ACS Nano* **2014**, *8*, 4033–4041.

(8) Qiao, J.; Kong, X.; Hu, Z.-X.; Yang, F.; Ji, W. High-Mobility Transport Anisotropy and Linear Dichroism in Few-Layer Black Phosphorus. *Nat. Commun,* **2014**, *4*.

(9) Kou, L.; Chen, C.; Smith, S. C. Phosphorene: Fabrication, Properties, and Applications. *J. Phys. Chem. Lett.* **2015**, *6*, 2794–2805.

(10) Keyes, R. The Electrical Properties of Black Phosphorus. *Phys. Rev.* **1953**, *92*, 580.

(11) Warschauer, D. Electrical and Optical Properties of Crystalline Black Phosphorus. *J. Appl. Phys.* **1963**, *34*, 1853–1860.

(12) Hohenberg, P.; Kohn, W. Inhomogeneous Electron Gas. *Phys. Rev.* **1964**, *136*, B864.

(13) Kohn, W.; Sham, L. J. Self-Consistent Equations Including Exchange and Correlation Effects. *Phys. Rev.* **1965**, *140*, A1133.

(14) Klimeš, J.; Michaelides, A. Perspective: Advances and Challenges in Treating van der Waals Dispersion Forces in Density Functional Theory. *J. Chem. Phys.* **2013**, *137*, 120901.

(15) Dion, M.; Rydberg, H.; Schröder, E.; Langreth, D. C.; Lundqvist, B. I. Van der Waals Density Functional for General Geometries. *Phys. Rev. Lett.* **2004**, *92*, 246401.

(16) Murray, E. D.; Lee, K.; Langreth, D. C. Investigation of Exchange Energy Density Functional Accuracy for Interacting Molecules. *J. Chem. Theory Comput.* **2009**, *5*, 2754–2762.

(17) Lee, K.; Murray, E. D.; Kong, L.; Lundqvist, B. I.; Langreth, D. C. Higher-Accuracy van der Waals Density Functional. *Phys. Rev. B* **2010**, *82*, 081101.

(18) von Lilienfeld, O. A.; Tavernelli, I.; Rothlisberger, U.; Sebastiani, D. Optimization of Effective Atom Centered Potentials for London Dispersion Forces in Density Functional Theory. *Phys. Rev. Lett.* **2004**, *93*, 153004.

(19) Grimme, S. Semiempirical GGA-Type Density Functional Constructed with a Long-Range Dispersion Correction. *J. Comput. Chem.* **2006**, *27*, 1787–1799.

(20) Tkatchenko, A.; Scheffler, M. Accurate Molecular van der Waals Interactions From Ground-State Electron Density and Free-Atom Reference Data. *Phys. Rev. Lett.* **2009**, *102*, 073005.

(21) Grimme, S.; Antony, J.; Ehrlich, S.; Krieg, H. A Consistent and Accurate Ab Initio Parametrization of Density Functional Dispersion Correction (DFT-D) for the 94 Elements H-Pu. *J. Chem. Phys.* **2010**, *132*, 154104.

(22) Kim, H. Effect of Van der Waals Interaction on the Structural and Cohesive Properties of Black Phosphorus. *J. Korean Phys. Soc.* **2014**, *64*, 547–553.

(23) Cascella, M.; Lin, I.-C.; Tavernelli, I.; Rothlisberger, U. Dispersion Corrected Atom-Centered Potentials for Phosphorus. *J. Chem. Theory Comput.* **2009**, *5*, 2930–2934.

(24) Wu, M.; Fu, H.; Zhou, L.; Yao, K.; Zeng, X. C. Nine New Phosphorene Polymorphs With Non-Honeycomb Structures: A Much Extended Family. *Nano Lett.* **2015**, *15*, 3557–3562.

(25) Bachhuber, F.; von Appen, J.; Dronskowski, R.; Schmidt, P.; Nilges, T.; Pfitzner, A.; Weihrich, R. The Extended Stability Range of Phosphorus Allotropes. *Angew. Chem. Int. Ed.* **2014**, *53*, 11629–11633.

(26) Shulenburger, L.; Baczewski, A.; Zhu, Z.; Guan, J.; Tománek, D. The Nature of the Interlayer Interaction in Bulk and Few-Layer Phosphorus. *Nano Letters* **2015**, DOI: 10.1021/acs.nanolett.5b03615.

(27) Böcker, S.; Häser, M. Covalent Structures of Phosphorus: A Comprehensive Theoretical Study. *Z. Anorg. Allg. Chem.* **1995**, *621*, 258–286.

(28) Pisani, C.; Maschio, L.; Casassa, S.; Halo, M.; Schütz, M.; Usvyat, D. Periodic Local MP2 Method for the Study of Electronic Correlation in Crystals: Theory and Preliminary Applications. *J. Comput. Chem.* **2008**, *29*, 2113.

(29) Usvyat, D.; Maschio, L.; Pisani, C.; Schütz, M. Second Order Local Møller-Plesset Perturbation Theory for Periodic Systems: the CRYSCOR Code. *Z. Phys. Chem.* **2010**, *224*, 441–454.

(30) Pisani, C.; Schütz, M.; Casassa, S.; Usvyat, D.; Maschio, L.; Lorenz, M.; Erba, A. CRYSCOR: A Program for the Post-Hartree–Fock Treatment of Periodic Systems. *Phys. Chem. Chem. Phys.* **2012**, *14*, 7615–7628.

(31) Usvyat, D.; Civalleri, B.; Maschio, L.; Dovesi, R.; Pisani, C.; Schütz, M. Approaching the Theoretical Limit in Periodic Local MP2 Calculations with Atomic-Orbital Basis Sets: the Case of LiH. *J. Chem. Phys.* **2011**, *134*, 214105.

(32) Grüneis, A. A Coupled Cluster and Explicitly Correlated Møller-Plesset Perturbation Theory Study of the Pressure Induced Phase Transition in the LiH Crystal. *J. Chem. Phys.* **2015**, *143*, 102816.

(33) M. Del Ben, J. Hutter, and J. VandeVondele, Second-Order Møller–Plesset Perturbation Theory in the Condensed Phase: An Efficient and Massively Parallel Gaussian and Plane Waves Approach. *J. Chem. Theory Comput.* **2012**, *8*, 4177–4188.

(34) Usvyat, D.; Maschio, L.; Schütz, M. Periodic Local MP2 Method Employing Orbital Specific Virtuals. *J. Chem. Phys.* **2015**, *143*, 102805.

(35) Yang, J.; Kurashige, Y.; Manby, F. R.; Chan, G. K. L. Tensor Factorizations of Local Second-Order Møller-Plesset Theory. *J Chem Phys* **2011**, *134*, 044123.

(36) Müller, C.; Usvyat, D. Incrementally Corrected Periodic Local MP2 Calculations: I.

The Cohesive Energy of Molecular Crystals. *J. Chem. Theory Comput.* **2013**, *9*, 5590–5598.

(37) Martinez-Casado, R.; Usvyat, D.; Maschio, L.; Mallia, G.; Casassa, S.; Ellis, J.; Schütz, M.; Harrison, N. M. Approaching an Exact Treatment of Electronic Correlations at Solid Surfaces: The Binding Energy of the Lowest Bound State of Helium Adsorbed on MgO(100). *Phys. Rev. B* **2014**, *89*, 205138.

(38) Usvyat, D. High Precision Quantum-Chemical Treatment of Adsorption: Benchmarking Physisorption of Molecular Hydrogen on Graphane. *J. Chem. Phys.* **2015**, *143*, 104704.

(39) Schütz, M. Low-Order Scaling Local Electron Correlation Methods. III. Linear Scaling Local Perturbative Triples Correction (T). *J. Chem. Phys.* **2000**, *113*, 9986–10001.

(40) Werner, H.-J.; Schütz, M. An efficient Local Coupled Cluster Method for Accurate Thermochemistry of Large Systems. *J. Chem. Phys.* **2011**, *135*, 144116.

(41) Masur, O.; Usvyat, D.; Schütz, M. Efficient and Accurate Treatment of Weak Pairs in Local CCSD (T) Calculations. *J. Chem. Phys.* **2013**, *139*, 164116.

(42) Schütz, M.; Masur, O.; Usvyat, D. Efficient and Accurate Treatment of Weak Pairs in Local CCSD (T) Calculations. II. Beyond the Ring Approximation. *J. Chem. Phys.* **2014**, *140*, 244107.

(43) Grimme, S. Improved Second-Order Møller-Plesset Perturbation Theory by Separate Scaling of Parallel- and Antiparallel-Spin Pair Correlation Energies. *J. Chem. Phys.* **2003**, *118*, 9095–9102.

(44) Dovesi, R.; Orlando, R.; Erba, A.; Zicovich-Wilson, C. M.; Civalleri, B.; Casassa, S.; Maschio, L.; Ferrabone, M.; De La Pierre, M.; D'Arco, P. et al. CRYSTAL14: A Program for the Ab Initio Investigation of Crystalline Solids. *Int. J. Quant. Chem.* **2014**,

(45) Werner, H.-J.; Knowles, P. J.; Knizia, G.; Manby, F. R.; Schütz, M. Molpro: A General–Purpose Quantum Chemistry Program Package. *Wiley Interdiscip. Rev.: Comput. Mol. Sci.* **2012**, *2*, 242–253.

(46) Weigend, F.; Ahlrichs, R. Balanced Basis Sets of Split Valence, Triple Zeta Valence and Quadruple Zeta Valence Quality for H to Rn: Design and Assessment of Accuracy. *Phys. Chem. Chem. Phys.* **2005**, *7*, 3297–3305.

(47) Kendall, R. A.; Dunning, T. H.; Harrison, R. J. Electron Affinities of the First-Row Atoms Revisited. Systematic Basis Sets and Wave Functions. *J. Chem. Phys.* **1992**, *96*, 6796–6806.

(48) Maschio, L.; Usvyat, D.; Schütz, M.; Civalleri, B. Periodic Local Møller–Plesset Second Order Perturbation Theory Method Applied to Molecular Crystals: Study of Solid NH_3 and CO_2 Using Extended Basis Sets. *J. Chem. Phys.* **2010**, *132*, 134706.

(49) Peterson, K. A.; Dunning, T. H. Accurate Correlation Consistent Basis Sets for Molecular Core–Valence Correlation Effects: The Second Row Atoms Al–Ar, and the First Row Atoms B–Ne Revisited. *J. Chem. Phys.* **2002**, *117*, 10548–10560.

(50) Brown, A.; Rundqvist, S. Refinement of the Crystal Structure of Black Phosphorus. *Acta Crystallogr.* **1965**, *19*, 684–685.

(51) Cartz, L.; Srinivasa, S. R.; Riedner, R. J.; Jorgensen, J. D.; Worlton, T. G. Effect of Pressure on Bonding in Black Phosphorus. *J. Chem. Phys.* **1979**, *71*, 1718–1721.

(52) Perdew, J. P.; Burke, K.; Ernzerhof, M. Generalized Gradient Approximation Made Simple. *Phys. Rev. Lett.* **1996**, *77*, 3865.

(53) Adamo, C.; Barone, V. Toward Reliable Density Functional Methods Without Adjustable Parameters: The PBE0 Model. *J. Chem. Phys.* **1999**, *110*, 6158–6170.

(54) Brandenburg, J. G.; Grimme, S. A Dispersion-Corrected Density Functional Theory Case Study on Ethyl Acetate Conformers, Dimer, and Molecular Crystal. *Theor. Chem. Acc.* **2013**, *132*, 1–6.

(55) Ehrlich, S.; Moellmann, J.; Reckien, W.; Bredow, T.; Grimme, S. System-Dependent Dispersion Coefficients for the DFT-D3 Treatment of Adsorption Processes on Ionic Surfaces. *ChemPhysChem* **2011**, *12*, 3414–3420.

(56) Kanaki, E.; Sansone, G.; Maschio, L.; Paulus, B. The Effect of Electron Correlation on the Adsorption of Hydrogen Fluoride and Water on Magnesium Fluoride Surfaces. *Phys. Chem. Chem. Phys.* **2015**, *17*, 18722–18728.

(57) Spanu, L.; Sorella, S.; Galli, G. Nature and Strength of Interlayer Binding in Graphite. **2009**, *103*, 196401.

(58) Tsang, D. K. L.; Marsden, B. J.; Fok, S. L.; Hall, G. Graphite Thermal Expansion Relationship For Different Temperature Ranges. *Carbon* **2005**, *43*, 2902–2906.

(59) Björkman, T.; Gulans, A.; Krasheninnikov, A. V.; Nieminen, R. M. van der Waals Bonding in Layered Compounds from Advanced Density-Functional First-Principles Calculations. *Phys. Rev. Lett.* **2012**, *108*, 235502.

(60) Castellanos-Gomez, A. Black Phosphorus: Narrow Gap, Wide applications. *J. Phys. Chem. Lett.* **2015**, *6*, 4280–4291.

(61) Girifalco, L. A.; Lad, R. A. Energy of Cohesion, Compressibility, and the Potential Energy Functions of the Graphite System. *J. Chem. Phys.* **1956**, *25*, 693–697.

(62) Benedict, L. X.; Chopra, N. G.; Cohen, M. L.; Zettl, A.; Louie, S. G.; Crespi, V. H. Microscopic Determination of the Interlayer Binding Energy in Graphite. *Chem. Phys. Lett.* **1998**, *286*, 490–496.

(63) Zacharia, R.; Ulbricht, H.; Hertel, T. Interlayer Cohesive Energy of Graphite From Thermal Desorption of Polyaromatic Hydrocarbons. *Phys. Rev. B* **2004**, *69*, 155406.

Graphical TOC Entry
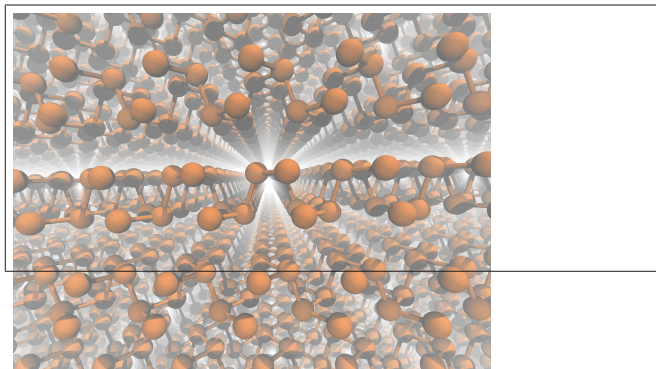
Black phosphorus, phosphorene, periodic quantum chemical methods, van der Waals interactions in solids